Experimental Study on Condensation Heat Transfer of R454B inside Small Diameter Microfin Tube

Afdhal Kurniawan Mainil

Hakimatul Ubudiyah

Naoki Sakamoto

Keishi Kariya

Akio Miyara

Experimental Study on Condensation Heat Transfer of R454B inside Small Diameter Microfin Tube

Afdhal Kurniawan MAINIL[1,*], Hakimatul UBUDIYAH [1], Naoki SAKAMOTO[1], Keishi KARIYA[2], Akio MIYARA[2,3]

[1]Graduate School of Science and Engineering, Saga University
Saga, Japan
Phone: +81-70-3982-9341, E-mail: mainilafdhalk@unib.ac.id

[2]Department of Mechanical Engineering, Saga University,
Saga, Japan
Phone: +81-952-28-8623, Fax: +81-952-28-8587, E-mail: miyara@me.saga-u.ac.jp

[3]International Institute for Carbon-Neutral Energy Research, Kyushu University,
Fukuoka, Japan

* Corresponding Author

ABSTRACT

The phase-down of the use of HFCs and high Global Warming Potential (GWP) refrigerants are accelerated all around the globe. R410A, which is currently widely used in HVAC&R systems, has a high GWP of 2088. Therefore, exploration of alternative refrigerants is needed to protect the global environment and in response to regulations related to the restriction of refrigerants with high GWP. R454B emerged as the top candidate for replacement because it has a GWP of 466 (78% reduction from R410A) with the properties and performance are close matches to that of R410A. R454B is a zeotropic mixture refrigerant made of R1234yf and R32 (31.1% and 68.9% in mass). However, the concern now is because this refrigerant is still classified as an A2L category, which is still mildly flammable. One proposed solution is to reduce the amount of refrigerant charge by applying it to a small diameter microfin tube. The present study examines the condensation heat transfer of R454 B inside a 3.5 mm OD horizontal microfin tube. The condensation heat transfer coefficient was measured for mass velocity ranging between 50 kg $m^{-2}s^{-1}$ and 200 kg $m^{-2}s^{-1}$, vapor quality from 0.1 to 0.9, and saturation temperature of around 20^{o}C. The effects of mass velocity and vapor quality were analyzed and discussed. The experimental data was compared to a correlation for pure refrigerants.

1. INTRODUCTION

The heating, ventilation, air conditioning, and refrigeration (HVAC&R) sector are currently evolving as it transitions away from hydrofluorocarbons (HFCs) as working fluids and continues to encourage environmentally friendly refrigerants with lower global warming potential (GWP). Some replacement candidates include hydro-fluoro-olefins (HFOs), and mixtures of HFCs/HFOs hope to mitigate the high GWP, as the requirements by international regulation. Nowadays, R410A is one of the most widely used refrigerants for air conditioning applications in worldwide (Zhao et al., 2015). It has a high GWP (2088(IPCC, 2007)); therefore, it will be phased out shortly by replacing it with the low GWP refrigerant (Mota-Babiloni et al., 2017). One promising candidate to replace R410A is R454B with a GWP of 466 (IPCC, 2007) (78 % reduction from R410A) with properties nearly identical to R410A (Devecioğlu, 2017; Shen et al., 2022; Tran et al., 2021). R454B is a zeotropic mixture refrigerant made of R1234yf and R32 (31.1% and 68.9% in mass). R454B has a relatively small temperature glide (around 1.5°C) compared to other mixture refrigerants that have same constituent components, such as R454C (approximately 7 °C) and R454A (approximately 5°C), as shown in figure 1 and figure 2.

However, the current concern is that R454B is categorized as A2L (ASHRAE, 2019), which is mildly flammable. In applying a heat exchanger that uses tubes, one potential option is to use a small diameter microfin tube that enhances heat transfer and reduces the amount of refrigerant charge.

This study investigated the two-phase flow condensation heat transfer of R454B inside a 3.5 mm OD microfin tube. The effects of mass velocity and vapor quality were analyzed and discussed. The condensation heat transfer coefficient is measured for mass velocity ranging between 50 kg $m^{-2}s^{-1}$and 200 kg $m^{-2}s^{-1}$, vapor quality from 0.1 to 0.9, and the saturation temperature around 20 °C. The obtained data was compared to a correlation for pure refrigerants.

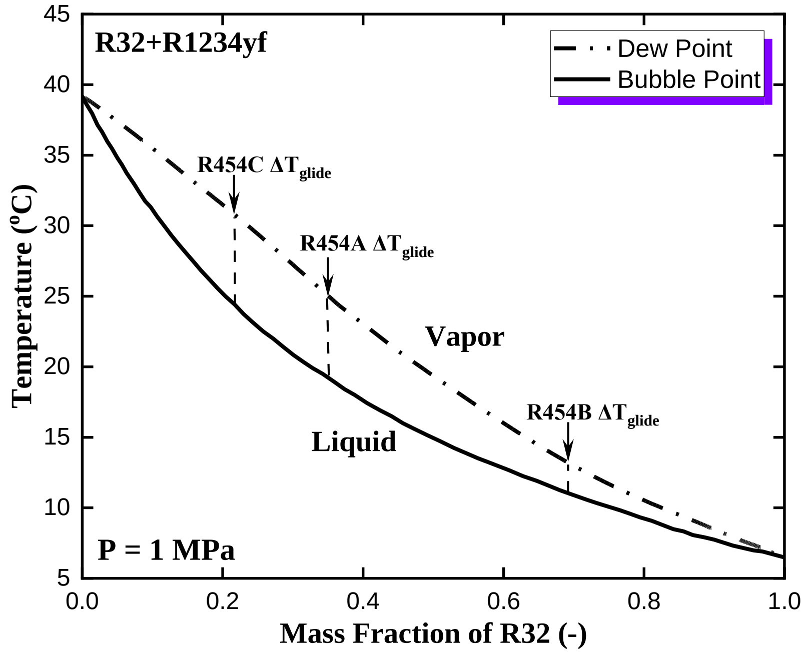

Figure 1: R32/R1234yf equilibrium diagram at a constant pressure equal to 1 MPa

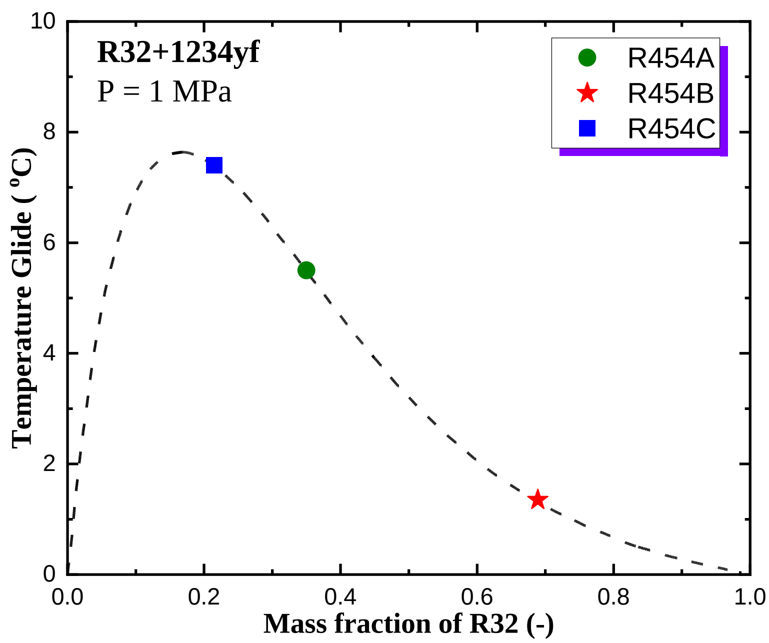

Figure 2: Temperature glide of R32/R1234yf mixture for various mass fraction

2. EXPERIMENTAL APPARATUS AND DATA REDUCTION

2.1 Experimental Apparatus

Figure 3 depicts a schematic of the experimental apparatus. The test equipment consists of two pumps, a Coriolis flowmeter, two preheaters, three mixing chambers, a test section, some water loops, an accumulator, a cooler, and a gas chromatograph. The two pumps are used to circulate the refrigerant; the difference between the two pumps is in the test conditions, with the first pump used for mass velocities of 50 kg m^2s^{-1} and lower and the second pump used for mass velocities more than 50 kg m^2s^{-1}. Three mixing chambers are installed at the inlet and outlet of the test section and the input of the first preheater to measure pressure and the bulk temperature of the refrigerant. The preheaters are adjusted to control the enthalpy of the refrigerant before entering the test section. The accumulator was applied to set the system pressure of the test apparatus. The cooler cools the refrigerant to ensure the refrigerant is in liquid form to recirculated as a cycle. Gas chromatography serves to determine the composition of the mixed refrigerant by measuring the mass fraction of each component forming the mixed refrigerant.

The experimental apparatus is also equipped with several K-type thermocouples installed in some positions to measure the refrigerant temperature. Besides, a sight glass is placed in the inlet and outlet of the test section to visualize the refrigerant, and a data logger is used to record all measuring instruments. The test equipment is also well insulated to maintain the system temperature.

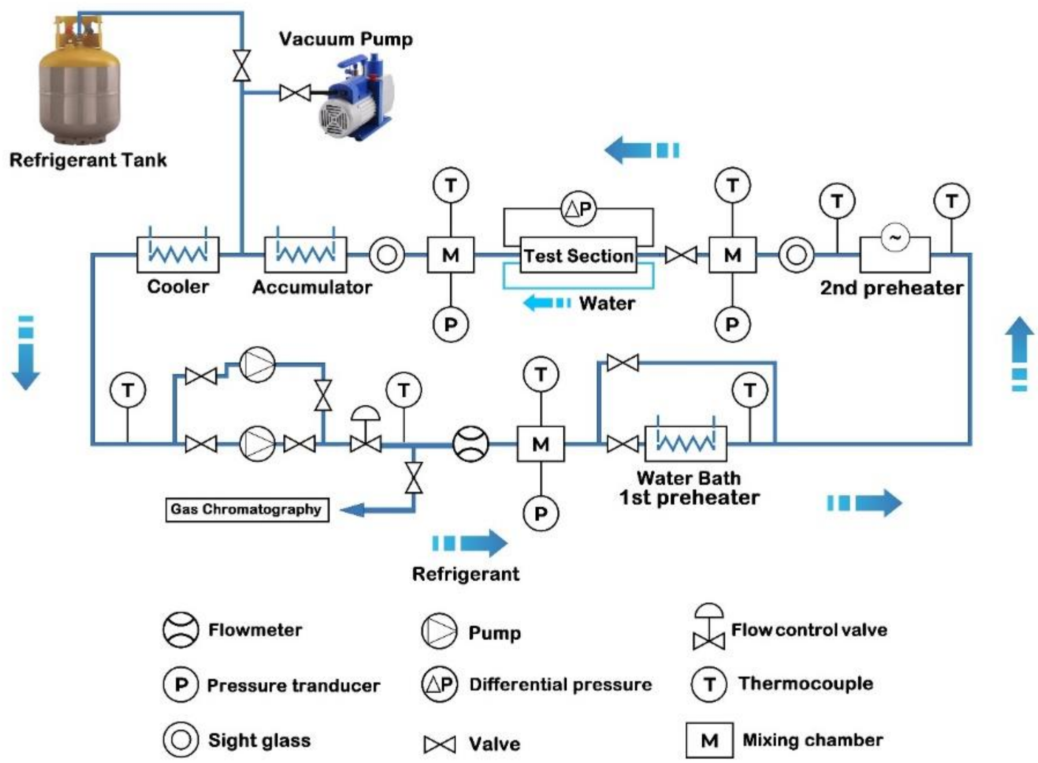

Figure 3: Experimental Apparatus

Figure 4 illustrates a schematic of the test section. A tube-in-tube was applied to transfer heat from the refrigerant to the water in the test section. The test section consists of a horizontally placed copper microfin tube, two headers, and three water channels. It has a total length of 852 mm and an effective heat transfer length of 744 mm. The wall temperature is measured using several T-type thermocouples installed on the test section's wall. The test tube is a small diameter microfin tube with 3.5 mm and 3.18 mm outer and equivalent diameter, respectively.

Figure 3 shows the photography and schematic view of microfin tube. The specification of microfin test tube is: number of fins is 25, apex angle (γ) is 35º, helix angle (θ) is 10º, tube wall thickness (δ) is 0.15 mm, fin height (h) is 0.10 mm, and an area expansion ratio (η) of 1.36. The equivalent diameter (d_{eq}) is 3.18 mm. The diameter indicates the equivalent diameter in the figure 3 with the help of the dashed line.

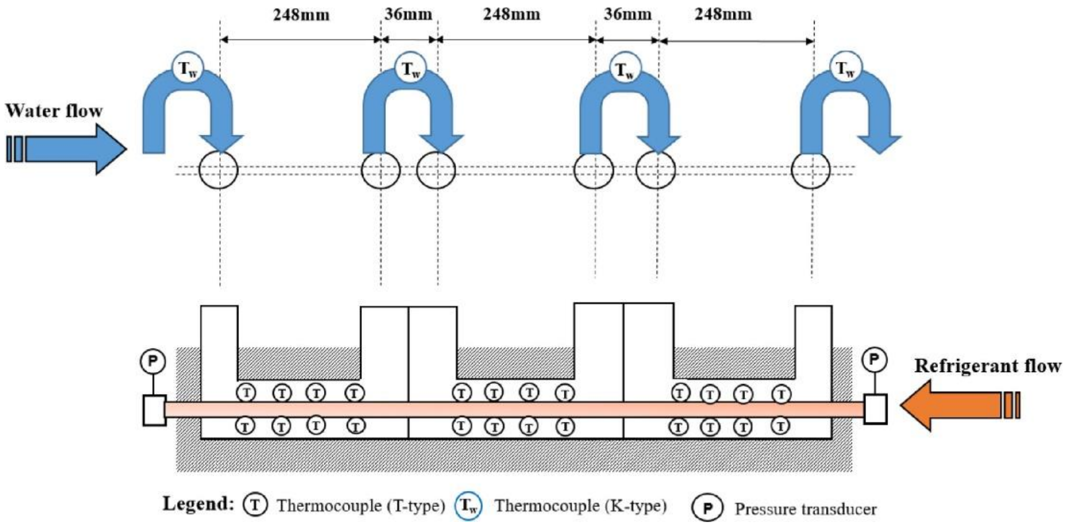

Figure 4: The test section details

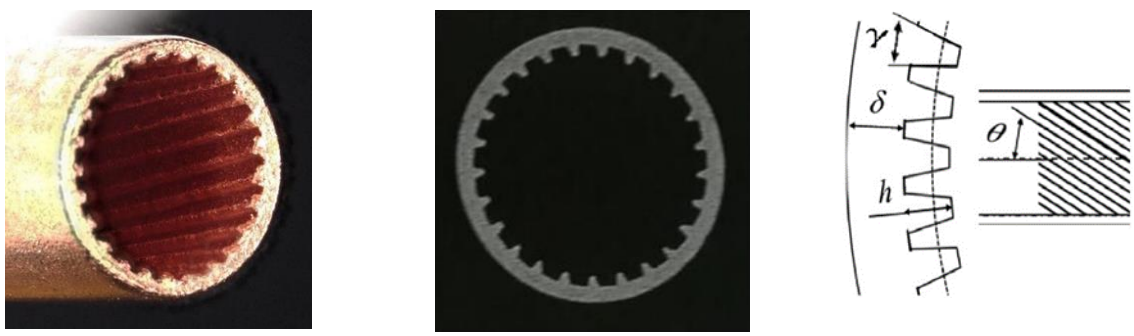

Figure 5: Photography and schematic view of the microfin tube

2.2 Data Reduction

The local condensation heat transfer coefficient during condensation is determine by the Equation (1).

$$\alpha = \frac{Q_{\mathrm{wat(i)}}}{\pi d_{\mathrm{eq}} Z_{\mathrm{(i)}} \left(T_{\mathrm{r(i)}} - T_{\mathrm{wi(i)}} \right)} \tag{1}$$

Where Q_{wat} , d_{eq}, $Z_{\mathrm{(i)}}$ and are the heat transfer rate of the water side of each sub-section, the equivalent diameter of the test tube (microfin) and the length of local point, respectively. T_{r} is refrigerant temperature that estimated from the measure refrigerant pressure, and T_{wi} is temperature of the inner wall of the test tube. The heat transfer rate amount of water side of each sub section can be calculated by Equation (2).

$$Q_{\mathrm{wat(i)}} = m_{\mathrm{wat}} \left(h_{\mathrm{wat(i)}} - h_{\mathrm{wat(i\text{-}1)}} \right) \tag{2}$$

In this case, the calculation of the microfin tube uses an equivalent diameter. The equivalent diameter (d_{eq}) is determined by Equation (3).

$$d_{\mathrm{eq}} = \sqrt{\frac{4A_{\mathrm{c}}}{\pi}} \tag{3}$$

The test tube's inner wall temperature is calculated from the measured temperature of the test tube is outside the wall surface by the one-dimensional equation of heat conduction Equation (4).

$$T_{\mathrm{wi(i)}} = T_{\mathrm{wo(i)}} + \frac{Q_{\mathrm{wat(i)}} \ln\left(\frac{d_{\mathrm{o}}}{d_{\mathrm{eq}}}\right)}{2\pi Z_{(\mathrm{i})} \lambda_{\mathrm{tube}}} \tag{4}$$

Where T_{wo} is the outside wall surface temperature, d_{o} is the outside diameter of the test tube, and λ is the thermal conductivity. Local enthalphy is calculated by Equation (5), and the vapor quality of refrigerant is calculated by Equation (6).

$$h_{(\mathrm{i})} = h_{(\mathrm{i\text{-}1})} - \left(\frac{Q_{\mathrm{wat(i)}}}{m_{\mathrm{r}}}\right) \tag{5}$$

$$x_{(\mathrm{i})} = \frac{h_{(\mathrm{i})} - h_{\mathrm{l}}}{h_{\mathrm{v}} - h_{\mathrm{l}}} \tag{6}$$

Where $h_{(\mathrm{i})}$ is the local enthalpy of refrigerant at each wall thermocouple point of the test tube, h_{l} and h_{v} are the saturated liquid and vapor enthalpy of refrigerant, respectively. Since R454B is a binary mixture of R32 (68.9 mass%) and R1234yf (31.1 mass%), the local refrigerant temperatures are calculated by the mixture component mass balance from equation 7, 8, and 9. The value of $\dot{m}_{\mathrm{b}}$, $\dot{m}_{\mathrm{l}}$ and $\dot{m}_{\mathrm{v}}$ represents the total mass flow rate, liquid-phase mass flow rate and the vapor-phase mass flow rate, respectively. w_{b}, w_{l}, and w_{v} are the bulk mass fraction, liquid phase, and vapor phase mass fractions of the binary mixture, respectively. The application of gas chromatography can know the bulk concentration of the binary temperature at the operating condition.

$$\dot{m}_{\mathrm{b}} w_{\mathrm{b}} = \dot{m}_{\mathrm{v}} w_{\mathrm{v}} + \dot{m}_{\mathrm{l}} w_{\mathrm{l}} \tag{7}$$

$$x = \frac{\dot{m}_{\mathrm{v}}}{\dot{m}} \tag{8}$$

$$w_{l} = \frac{w_{\mathrm{b}}}{1 + x\left(\frac{w_{\mathrm{v}}}{w_{\mathrm{l}}} - 1\right)} \tag{9}$$

The refrigerant temperature, T_r, were obtained from REFPROP 10.0a (Lemmon et al., 2018) with the function follows:

$$w_{\mathrm{v}} = f\left(w_{\mathrm{l}}, P\right) \tag{10}$$

$$T_r = f\left(w_{\mathrm{l}}, P\right) \tag{11}$$

The corresponding enthalpy for liquid and vapor phase is also evaluated from REFPROP 10.0a (Lemmon et al., 2018) by the function of the concentration and the pressures at the measurement point.

$$h_l = f\left(w_l, P\right) \tag{12}$$

$$h_v = f\left(w_v, P\right) \tag{13}$$

3. RESULT AND DISCUSSION

Figure 6 shows the effect of mass velocity and vapor quality on condensation heat transfer coefficient at the saturation temperature of around 20 °C. Three different mass velocities of 50, 100, and 200 kg $m^{-2}s^{-1}$ were varied. . It was shown that the heat transfer coefficient increases with increased vapor quality and mass velocity. The velocity of vapor and liquid phases have been shown to be high at high vapor quality, resulting in high shear stress at the interface between vapor and liquid film relative to low vapor quality. There is a related rise in the heat transfer coefficient due to the increased interfacial shear stress. It is found that the heat transfer coefficient increases as vapor quality changes from 0.07 to 0.98. The heat transfer coefficient of R454B over the given vapor quality range increases from 2.1 to 14.9 kW m^{-2} K^{-1} with the increase in mass velocity from 50 to 200 kg m^{-2} s^{-1}.

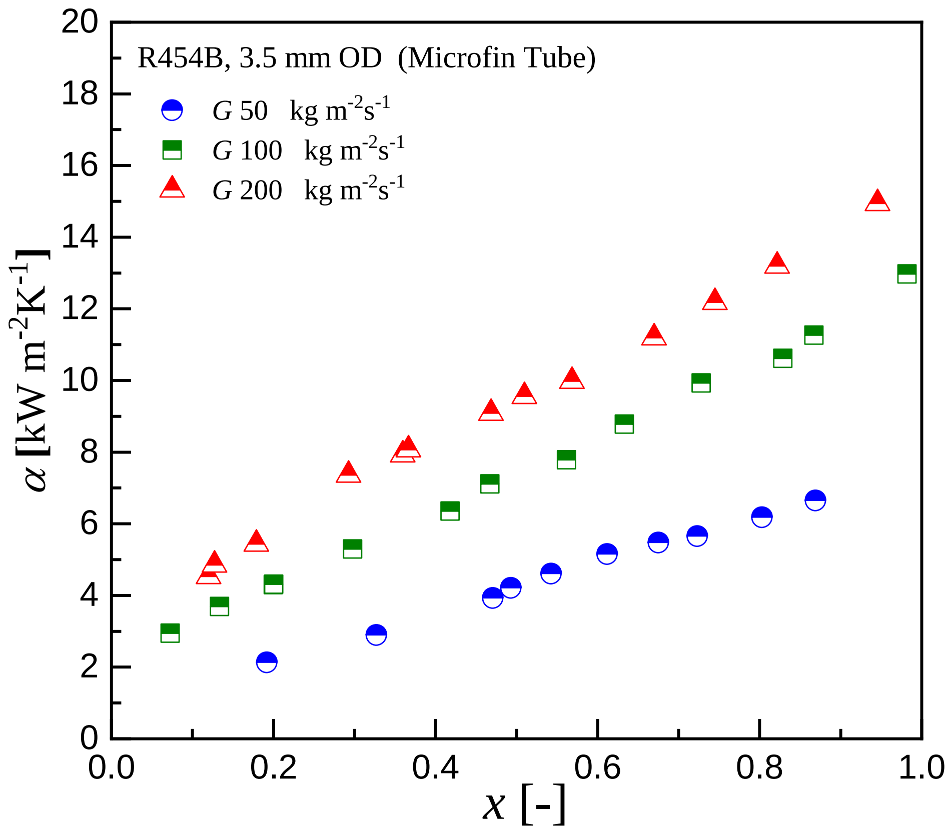

Figure 6: Relation between heat transfer coefficient and vapor quality at different mass velocity

Figure 7 compares the heat transfer coefficient of R454B with pure refrigerant R1234yf taken from (Mainil et al., 2022) with the same mass velocity and tube specifications. The figure shows that HTC's R454B is slightly larger than R1234yf, increasing 1.1 to 1.4 times enhancement. With a sizeable R32 composition of about 68.9% in R454B, HTC's increase is relatively small. The condition is because of the degradation of HTC due to mass transfer resistance due to the presence of a temperature glide of zeotropic mixture refrigerant.

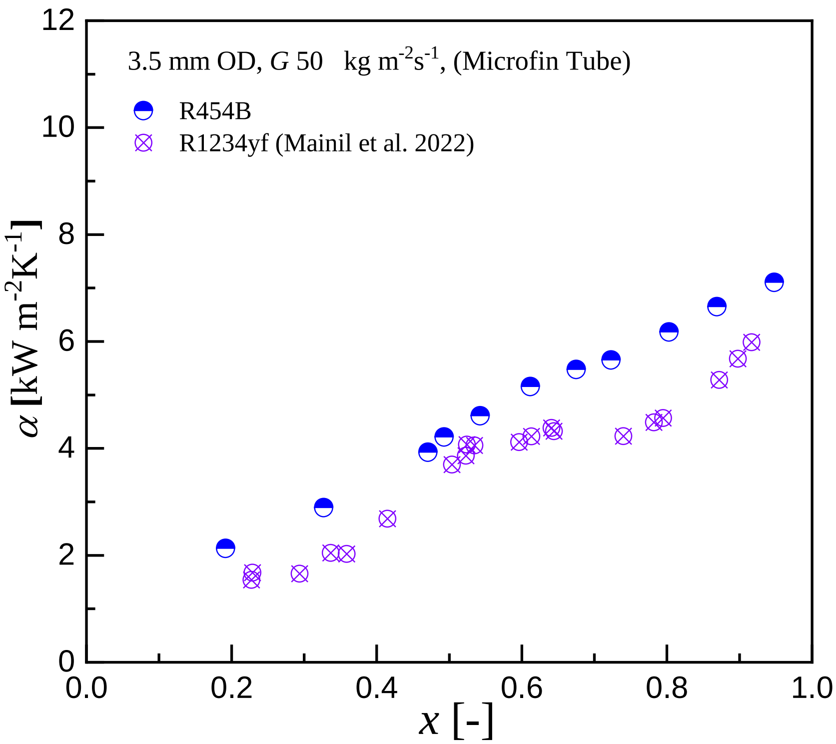

Figure 7: Relation between heat transfer coefficient and vapor quality at different refrigerant

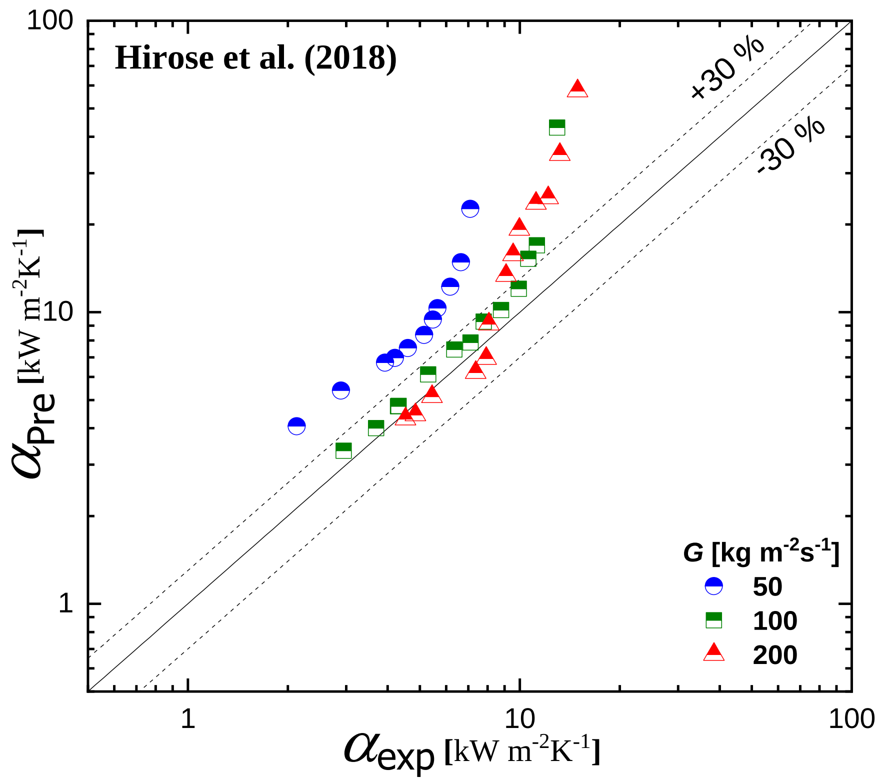

Figure 8: Comparison of measured and predicted heat transfer coefficient values by (Hirose et al., 2018)

Figure 8 shows the comparison between the experimental heat transfer coefficient and heat transfer coefficient from the correlation using the condensation heat transfer model developed by (Hirose et al., 2018). This correlation majority is not well predicted and majority overestimated with average deviation (AD), and the mean absolute deviation (MD) is 64% and 67%, respectively, calculated using equations 14 and 15. The predictive model of (Hirose et al., 2018) was developed using experimental data using microfin tube, where the diameter is close to this study, where the equivalent diameter is 3.48 mm. However, the estimation results show that the majority of the prediction results are larger than the experimental results. The condition is because the prediction model was developed using pure refrigerants. Therefore, it can be concluded that there is a degradation of this heat transfer coefficient compared to a pure refrigerant. This degradation is caused by the mass transfer resistance of the zeotropic refrigerant.

$$AD = \frac{1}{n}\sum_{i=n}^{n}\left(\frac{\alpha_{\mathrm{pre}} - \alpha_{\mathrm{exp}}}{\alpha_{\mathrm{exp}}}\right)\times 100 \tag{14}$$

$$MD = \frac{1}{n}\sum_{i=n}^{n}\left|\frac{\alpha_{\mathrm{pre}} - \alpha_{\mathrm{exp}}}{\alpha_{\mathrm{exp}}}\right|\times 100 \tag{15}$$

4. CONCLUSIONS

Experiments were carried out to investigate the condensation heat transfer of R454B in a horizontal microfin tube with an outer diameter of 3.5 mm. The experimental results for heat transfer were analyzed. The conclusions of this study are as follows:

- The heat transfer coefficient was increased with an increased vapor quality and mass velocity. The HTC of R454B increases from 2.1 to 14.9 kW m^{-2} K^{-1} when vapor quality changes from 0.07 to 0.98 and three different mass velocities of 50, 100, and 200 kg $m^{-2}s^{-1}$.
- The velocity of vapor and liquid phases have been shown to be high at high vapor quality, resulting in high shear stress at the interface between vapor and liquid film relative to low vapor quality. There is a related rise in the heat transfer coefficient due to the increased interfacial shear stress.
- The HTC's R454B is slightly larger than R1234yf, increasing 1.1 to 1.4 times enhancement. With a sizeable R32 composition of about 68.9% in R454B, HTC's increase is relatively small. The condition is because of the degradation of HTC due to mass transfer resistance due to the presence of a temperature glide of zeotropic mixture refrigerant.
- A correlation for pure refrigerants (Hirose et al., 2018) does not well predicted the heat transfer coefficient of R454B and majority overestimated with average deviation (AD), and the mean absolute deviation (MD) is 64% and 67%, respectively. Therefore, it can be concluded that there is a degradation of this heat transfer coefficient compared to a pure refrigerant. This degradation is caused by the mass transfer resistance of the zeotropic refrigerant.

NOMENCLATURE

A	Cross sectional area	(m^2)
d	Diameter	(m)
G	Mass velocity	(kg m^{-2} s^{-1})
h	Enthalpy	(kJ kg^{-1})
m	Mass flow rate	(kg s^{-1})
P	Pressure	(MPa)
Q	Heat transfer rate	(W)

T	Temperature	(ºC)
x	Vapor quality	(-)
w	Mass fraction	
z	Effective heat transfer length	(m)

Greek symbols

α	Heat transfer coefficient	(kW m^{-2} K^{-1})
λ	Thermal conductivity	(kW m^{-1} K^{-1})
η	Expansion ratio	(-)
θ	Helix angle	(deg)
δ	Tube wall thickness	(mm)
γ	Apex angle	(deg)

Subscript

b	Bulk
eq	Equivalent
exp	Experiment
i	Inner
l	Liquid
o	Outer
pre	Predicted
r	Refrigerant
v	Vapor
w	Wall
wat	Water

REFERENCES

ASHRAE. (2019). Designation and Safety Classification of Refrigerants. *ANSI/ASHRAE Standard 34-2019*, *2019*(34), 1–52. www.ashrae.org

Devecioğlu, A. G. (2017). Seasonal performance assessment of refrigerants with low GWP as substitutes for R410A in heat pump air conditioning devices. *Applied Thermal Engineering*, *125*, 401–411. https://doi.org/10.1016/j.applthermaleng.2017.07.034

Hirose, M., Ichinose, J., & Inoue, N. (2018). Development of the general correlation for condensation heat transfer and pressure drop inside horizontal 4 mm small-diameter smooth and microfin tubes. *International Journal of Refrigeration*, *90*, 238–248. https://doi.org/10.1016/j.ijrefrig.2018.04.014

IPCC 2007. (2007). *Climate Change 2007: The Physical Science Basis. Contribution of Working Group I to the Fourth Assessment Report of the Intergovernmental Panel on Climate Change. Summary for Policymakers. (Edited by Solomon, S. DQin MManning ZChen MMarquis KAveryt MHL MS* (p. 996).

Lemmon, E. W., Bell, I. H., Huber, M. L., & McLinden, M. O. (2018). *NIST Standard Reference Database 23: Reference Fluid Thermodynamic Properties-REFPROP (DLL Version 10.0a). NIST, USA.*

Mainil, A. K., Sakamoto, N., Ubudiyah, H., Kariya, K., & Miyara, A. (2022). Experimental Investigation on Condensation Heat Transfer of Refrigerant R1234yf in Horizontal Microfin Tube. *Transaction of the Japan Society of Refrigeration and Air Conditioning Engineers*, *39*(2).

Mota-Babiloni, A., Makhnatch, P., & Khodabandeh, R. (2017). Recent investigations in HFCs substitution with lower GWP synthetic alternatives: Focus on energetic performance and environmental impact Adrián. *International Journal of Refrigeration*, *82*, 288–301. https://doi.org/10.1016/j.ijrefrig.2017.06.026

Shen, B., Li, Z., & Gluesenkamp, K. R. (2022). Experimental study of R452B and R454B as drop-in replacement for R410A in split heat pumps having tube-fin and microchannel heat exchangers. *Applied Thermal Engineering*, *204*(December 2021), 117930. https://doi.org/10.1016/j.applthermaleng.2021.117930

Tran, N., Kasireddy, R. V., & Wang, C. C. (2021). An experimental investigation on convective boiling heat transfer of R-454B with lubricant oil of POE-32 or POE-68 mixture in a horizontal smooth tube. *International Journal of Heat and Mass Transfer*, *181*, 121990. https://doi.org/10.1016/j.ijheatmasstransfer.2021.121990

Zhao, L., Zeng, W., & Yuan, Z. (2015). Reduction of potential greenhouse gas emissions of room air-conditioner refrigerants: A life cycle carbon footprint analysis. *Journal of Cleaner Production*, *100*, 262–268. https://doi.org/10.1016/j.jclepro.2015.03.063

ACKNOWLEDGEMENT

The Japan Copper Development Association financially supported this study. We wish to express our gratitude for their financial support. AKM would like to express special appreciate to Strategic International Postgraduate Program (SIPOP) Saga University for Ph.D. Scholarship.